RESEARCH ARTICLE

Three-dimensional visualization of the functional fascicular groups of a long-segment peripheral nerve

Jian Qi[1,#], Wei-Ya Wang[2,#], Ying-Chun Zhong[3], Jia-Ming Zhou[4], Peng Luo[5], Ping Tang[3], Cai-Feng He[6], Shuang Zhu[7], Xiao-Lin Liu[1], Yi Zhang[8,*]

1 Department of Orthopedics and Microsurgery, First Affiliated Hospital of Sun Yat-sen University, Guangzhou, Guangdong Province, China
2 Department of Plastic Surgery, Nanxishan Hospital of Guangxi Zhuang Autonomous Region, Guilin, Guangxi Zhuang Autonomous Region, China
3 Automation College, Guangdong University of Technology, Guangzhou, Guangdong Province, China
4 Scientific Research Department, Sixth Affiliated Hospital of Sun Yat-sen University, Guangzhou, Guangdong Province, China
5 Department of Orthopedics, Shenzhen Nanshan People's Hospital, Shenzhen, Guangdong Province, China
6 Zhongshan University Medical Equipment Co., Ltd., Guangzhou, Guangdong Province, China
7 Department of Joint and Orthopedics, Orthopedic Center, Zhujiang Hospital of Southern Medical University, Guangzhou, Guangdong Province, China
8 Department of Plastic Surgery, First Affiliated Hospital of Sun Yat-sen University, Guangzhou, Guangdong Province, China

Funding: *This study was supported by the National Natural Science Foundation of China, No. 30571913; a grant from the Science and Technology Project of Guangdong Province of China, No. 2013B010404019; the Natural Science Foundation of Guangdong Province of China, No. 9151008901000006; the Medical Scientific Research Foundation of Guangdong Province of China, No. A2009173.*

Graphical Abstract

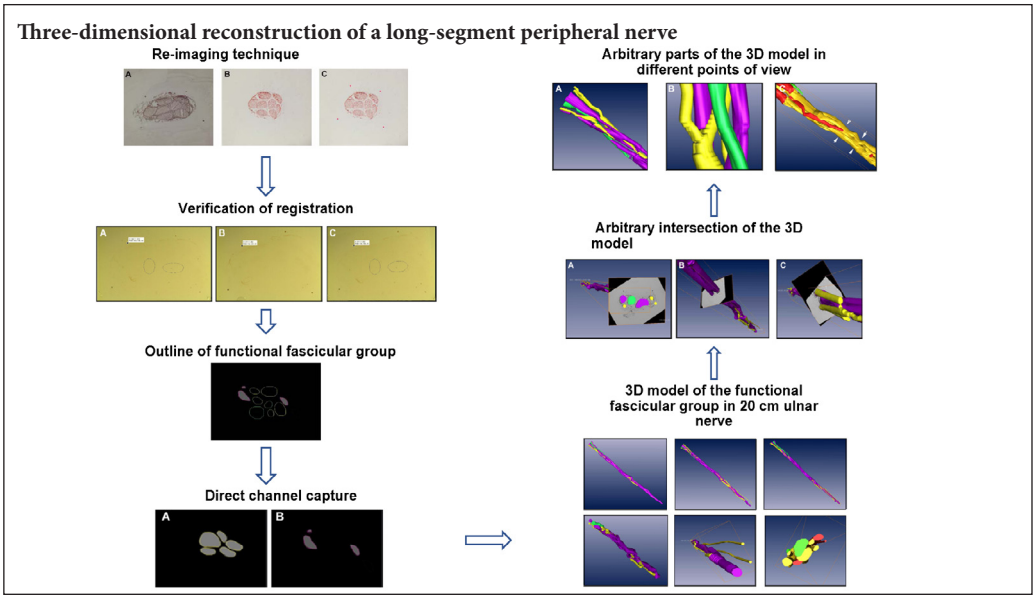

Correspondence to:
Yi Zhang, M.D., Ph.D., doczy2006@126.com.

#These authors contributed equally to the paper.

orcid:
0000-0001-6463-6970 (Yi Zhang)

doi: *10.4103/1673-5374.235307*

Accepted: *2018-05-13*

Abstract

The three-dimensional (3D) visualization of the functional bundles in the peripheral nerve provides direct and detailed intraneural spatial information. It is useful for selecting suitable surgical methods to repair nerve defects and in optimizing the construction of tissue-engineered nerve grafts. However, there remain major technical hurdles in obtaining, registering and interpreting 2D images, as well as in establishing 3D models. Moreover, the 3D models are plagued by poor accuracy and lack of detail and cannot completely reflect the stereoscopic microstructure inside the nerve. To explore and help resolve these key technical problems of 3D reconstruction, in the present study, we designed a novel method based on re-imaging techniques and computer image layer processing technology. A 20-cm ulnar nerve segment from the upper arm of a fresh adult cadaver was used for acetylcholinesterase (AChE) staining. Then, 2D panoramic images were obtained before and after AChE staining under the stereomicroscope. Using layer processing techniques in Photoshop, a space transformation method was used to fulfill automatic registration. The contours were outlined, and the 3D rendering of functional fascicular groups in the long-segment ulnar nerve was performed with Amira 4.1 software. The re-imaging technique based on layer processing in Photoshop produced an image that was detailed and accurate. The merging of images was accurate, and the whole procedure was simple and fast. The least square support vector machine was accurate, with an error rate of only 8.25%. The 3D reconstruction directly revealed changes in the fusion of different nerve functional fascicular groups. In conclusion. The technique is fast with satisfactory visual reconstruction.

Key Words: *nerve regeneration; peripheral nerve; ulnar nerve; three-dimensional reconstruction; functional fascicular group; registration; segmentation; locating spots; auto-registration; acetylcholinesterase; neural regeneration*

Introduction

The evolution from two-dimensional (2D) medical imaging to three-dimensional (3D) visualization has become a hot topic with the development of medical imaging and computer-assisted techniques. The 3D visualization of functional fascicular groups inside peripheral nerves can provide detailed 3D information on functional fascicles and fascicular groups, thereby providing crucial information for nerve rehabilitation in the clinical setting as well as the 3D construction of artificial nerves (Pommert et al., 2006; Ren and Pei, 2009; Sun et al., 2009). However, there remain technical problems that need to be solved for 3D visualization, including the acquisition of 2D panoramic images with locating spots, registration, identification and 3D reconstruction of the nerve groups. These procedures also require a great deal of time and manual effort. The biggest limitation is that the visualized spatial model is not accurate enough, which affects the reconstruction of the 3D microstructure of the nerves, as well as the detailed structure of the peripheral nerve.

Therefore, the present study focused on the key technical limitations during 3D reconstruction of peripheral nerves, such as the acquisition of panoramic images and computerized automatic image registration for serial slices. This study also tested the feasibility of third party software, such as Amira, in 3D reconstruction.

Materials and Methods

Materials

A fresh sample of ulnar nerve from the upper arm was obtained within 24 hours after the death of a 35-year-old male donor who died from head injury in a car accident, without any lesions or tumors in the limb. The family of the deceased was approved by the Shenzhen Red Cross in China to donate the dead body (registration date: 2013-06-01). The family donated the body to the First Affiliated Hospital of Sun Yat-sen University of China (donation date: 2013-06-09) for clinical research. The family members of the deceased were aware of the details of the study and signed informed consent. Ethical approval was granted by the First Affiliated Hospital of Sun Yat-sen University of China (approval No. [2013]A-065).

Sample preparation and fixation

A 20-cm-long ulnar nerve segment from the transverse striation at the top of the armpit to the internal epicondyle of the humerus was excised. The nerve segment had a width of 4.7 mm (external–internal) and a thickness of 2.8 mm (anteroposteriorly) at the proximal end, and a width of 4.0 mm (external–internal) and thickness of 3.2 mm (anteroposteriorly) at the distal end. The sample was then prepared and fixed. Briefly, the fatty tissue around the epineurium was removed, and the sample was placed on a soft wooden board with both ends pinned to prevent curling and deformation. Four strands of hair from an adult female (approximately 0.08 mm in diameter) were placed along the nerve on four sides parallel to its longitudinal axis, and fixed in 10% formalin solution and then embedded in paraffin for 2 hours to help keep the hair straight without curling or shifting. Afterwards, the sample was embedded in optimal cutting temperature compound and stored at −80°C for one week before analysis.

Sample slicing

The nerve sample was transected into 20-mm segments at −20°C, vertically embedded in optimal cutting temperature compound, and then horizontally sliced into 400 consecutive 15-μm-thick slices with an interval of 0.5 mm on a freezing microtome (Leica CM1850 UV, Leica Biosystems, Wetzlar, Germany). All slices were placed on siliconized slides with sequences marked.

Staining

The slices were stained for acetylcholinesterase (AChE) using the Karnovsky–Roots copper hexacyanoferrate method to facilitate discrimination of different functional groups in 2D images. The staining reagent contained the following: acetylthiocholine iodide (Sigma-Aldrich, St. Louis, MO, USA) 100 mg; 0.1 M phosphate-buffered saline (PBS) solution 128 mL, containing 0.1 M dibasic sodium phosphate (Guangzhou No. 2 Chemical Reagent Factory, Guangzhou, China) 18 mL; 0.1 M potassium phosphate monobasic (Guangzhou No. 2 Chemical Reagent Factory) 14 mL; 0.1 M sodium citrate (Guangzhou No. 2 Chemical Reagent Factory) 8 mL; 30 mM copper sulfate (Tianjin Yongda Chemical Reagent Development Center, Tianjin, China) 20 mL; 5 mM potassium ferricyanide (Tianjin Yongda Chemical Reagent Development Center) 20 mL; and distilled water 16 mL. The solution was prepared 20 minutes in advance.

Within 4 hours of slicing, the slices were immersed in staining solution and placed in a 4°C refrigerator for 24 hours. The slices were then taken out and air-dried. Excessive deposition was rinsed off with PBS at 4°C. The slices were dehydrated in 95% alcohol and anhydrous alcohol, one minute each, and then treated with dimethyl benzene for three minutes. Finally, the slices were air dried and mounted in neutral gum.

Acquisition of 2D panoramic images

Using re-imaging techniques, 800 slices before and after staining were photographed on a stereomicroscope (Z61; Olympus, Tokyo, Japan) using MSHOT MD90 micro-digital imaging equipment (Guangzhou Mingmei Technology Co., Ltd., Guangzhou, China). The 2D panoramic images were acquired using Mingmei software (image auto-splicing software) and saved with the following parameters: 3488 × 2616 pixels, 1.5 × 4.0 optical zoom, 24-bit color model, 72 × 72 dpi JPG format file, with a size of 500 kB each, 400 MB in total.

2D panoramic images with indication spots

The 2D panoramic image layers before and after AChE staining were registered in line with the contours of nerve bundles using the layering technique in Photoshop CS2 (Adobe, San Jose, CA, USA). Four round spots were marked

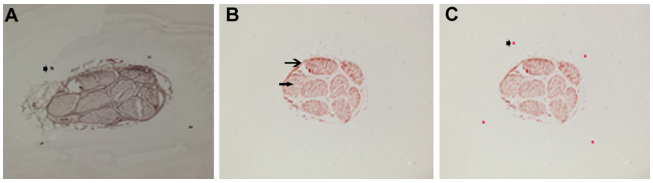

Figure 1 Re-imaging technique.
(A) Before AChE staining. (B) After AChE staining. (C) After Photoshop layer processing. AChE staining was used to recognize differences among functional fascicular groups. The long arrow indicates motor dominance bundles with deep staining. The long triangular arrow indicates sensory dominance bundles with light staining. The short triangular arrows indicate locating points. Photoshop layer processing was used, and locating points were obtained. AChE: Acetylcholinesterase.

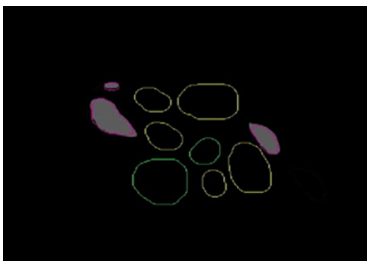

Figure 3 Obtaining the outline of functional fascicular group directly in Amira 4.1 software, and the data channel establishment of different fascicular groups.
Red area: Compound bundles of sensory dominance; green area: compound bundles of motor dominance; yellow area: compound bundles.

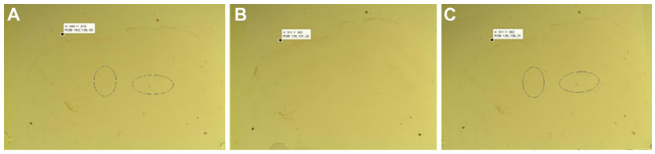

Figure 2 Verification of registration.
(A) The image before registration: Two oval spots served as marks. (B) The standard image. (C) The registered image for A and B.

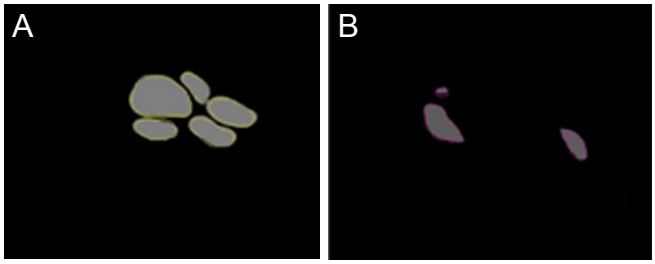

Figure 4 Direct channel captured in Amira 4.1 software.
(A) Compound bundle channels. (B) Compound bundle channels of sensory dominance.

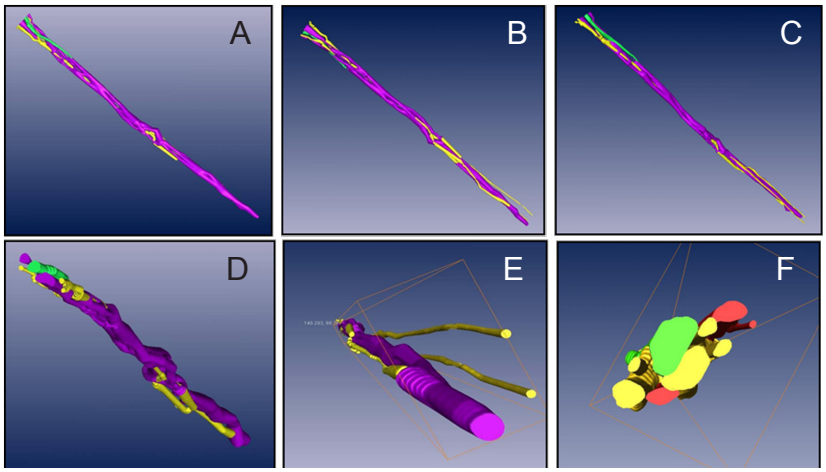

Figure 5 Arbitrary points of view (A, B, C) of the three-dimensional model of the functional fascicular group in a 20-cm ulnar nerve segment of the upper limb in horizontal axis (X axis, D), coronal axis (Y axis, E) and sagittal axis (Z axis, F).
Reconstructed long ulnar nerve functional bundle of the upper arm can be visualized as a three-dimensional structure, which can be cut from different angles of view, at any cross-section or locally. Red area: Compound bundles of sensory dominance; green area: compound bundles of motor dominance; yellow area: compound bundles. The three-dimensional visualization structure can be observed from various angles.

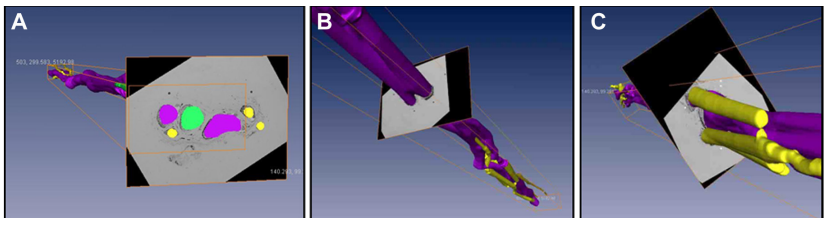

Figure 6 Images of arbitrary intersection of the three-dimensional model.
The three-dimensional model can almost fit the original two-dimensional image. (A) The 10th layer from the distal end. (B) The 145th layer from the distal end. (C) The 240th layer from the distal end. Reconstructed long ulnar nerve functional bundle of the upper arm can be visualized as a three-dimensional structure, which can be cut from different angles of view, at any cross-section or locally. Red area: Compound bundles of sensory dominance; green area: compound bundles of motor dominance; yellow area: compound bundles.

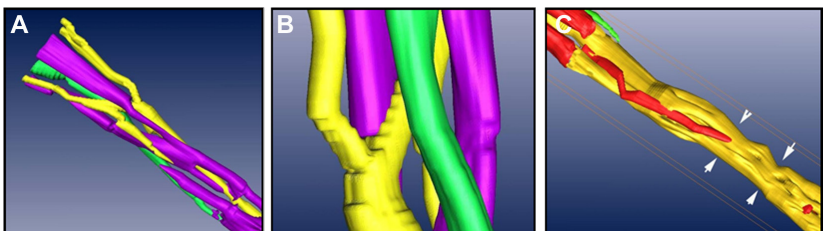

Figure 7 Arbitrary parts of the three-dimensional model from different points of view.
The right image shows the two places where the functional fascicular groups merge. (A) The 1st–68th layers from the distal end. (B) The 35th–54th layers from the distal end. (C) The 182nd–200th layers from the distal end. Red area: Compound bundles of sensory dominance; green area: compound bundles of motor dominance; yellow area: compound bundles.

manually according to the location and size of the adult hairs that were placed as locating marks before staining. The panoramic images with adult hairs as indication spots were deleted. In the end, 400 recomposed panoramic images with four marked indication spots were obtained.

Image registration and segmentation

Image registration: Four locating spots were recognized by optimized least square support vector machine (optimized LS–SVM), together with functions of stretching and shifting in computer-supported image processing. The images were processed and registered using external control points. A total of 400 panoramic images after AChE staining were obtained. The recognition accuracy of the four locating spots was verified by comparing the results with those obtained by normal LS–SVM and by radial basis function neural network.

Image segmentation: The images were processed using improved coarse K-means clustering method after AChE staining, which organizes pixel spots in proximity to each other with similar grayscale shades into separate groups. The serial boundaries of functional groups were obtained using gradient vector flow model. However, because this algorithm cannot automatically differentiate individual fascicular groups, and the automatic contour segmentation lacks precision, the fascicular groups had to be distinguished manually according to differences in AChE staining features when 3D reconstruction was performed with Amira 4.1 software (TGS, Bordeaux, France).

3D reconstruction

Compared with the original 2D images, every functional fascicular group was distinguished after registration and segmentation. The results indicated that the ulnar nerves from the upper arm did not have branches, and that the fascicular groups were compound bundles. Those groups that were deeply and uniformly stained were likely compound bundles composed mostly of sympathetic fibers. Moreover, those groups in which the AChE-positive areas were spotted were likely compound bundles with motor fibers. Those groups in which staining appeared solid or spotted were classified as compound bundles. Data channels were constructed for fascicular groups with different characteristics.

All different data channels were delivered to the 3D reconstruction Amira 4.1 software (TGS). At this stage, each channel was processed individually, and the three different data channels were combined to complete the whole 3D reconstruction, displaying the stereoscopic running and variation of functional fascicular groups with different characteristics. Furthermore, the zigzag boundaries were deleted and optimized by functions in Amira 4.1 software to achieve the best reconstruction.

Results

Acquisition of 2D panoramic images with full locating spots after being processed by re-imaging techniques and Photoshop software

Each nerve slice was photomicrographed with a stereomicroscope (Z61; Olympus) and MSHOT MD90 digital imaging equipment before and after the AChE staining. The image before staining was clear with complete and accurate locating spots, and the nerve contour was clear. After staining, although the contour was clear, the locating spots were either missing or had shifted. When the images before and after staining were uploaded into Photoshop, the contours were matched to a great extent. Moreover, the locating spots were accurate. A final picture could be obtained in as fast as 30 seconds with satisfactory results (**Figure 1**).

Verification of the registration algorithm

All nerve slices were registered using the registration algorithm. **Figure 2A** shows the image before registration, in which two oval spots served as marks. **Figure 2B** shows the standard image. **Figure 2C** displays the registered image after the image in **Figure 2A** and **B** are registered. The differences between the coordinates of pixels in **Figure 2A** and **B** are quite obvious. However, the coordinates are exactly the same after registration in **Figure 2B** and **C**, which indicates a successful registration.

Accuracy of registration: 400 2D images of serial histological sections from the ulnar nerve in sectional view (20 cm in length, with an interval of 0.5 mm) were registered by optimized LS–SVM. The error rate was 8.25%, which is more accurate than the 11.375% obtained with normal LS–SVM and the 14.75% of radial basis function neural network.

3D reconstruction of functional fascicular groups inside the long-segment peripheral nerve

On original 2D panoramic images, we observed three kinds of nerve bundles: compound bundles, compound bundles of motor dominance, and compound bundles of sensory dominance, most of which were compound bundles. Three channels were constructed after the original registered images were input into Amira 4.1 software, one for each distinct nerve bundle: the compound bundle in yellow; the compound bundle of sensory dominance in red; and the compound bundle of motor dominance in green (**Figure 3**). Direct channel was captured in Amira 4.1 software individually so that the crossing and merging of the different bundles could be distinguished after the 3D reconstruction (**Figure 4**). The 3D visualization structure could be observed from various angles (**Figure 5**). The 3D model from an arbitrary point of view is shown in **Figure 6**, and the 3D model from a different point of view is shown in **Figure 7**. These figures show the course of the ulnar nerve in the upper limb.

Discussion

It is known that the regeneration of the damaged nerve after peripheral nerve injury is the key to functional recovery. Optimal regeneration can be achieved by accurately matching each functional bundle to provide the best channels for the growth of regenerating axons. In this study, we aimed to establish a 3D model of functional bundles in the human ulnar nerve, and to investigate the relationship among them. This may help achieve precise functional bundle anastomo-

ses for repairing nerve injur, and also provide a visual 3D spatial reference for the construction of the internal spatial structure of tissue-engineered nerve bridges. However, some technical problems still need to be solved for 3D visualization, including the acquisition of 2D panoramic images with locating spots, registration, identification and 3D reconstruction of the nerve groups.

3D reconstruction of internal fascicular groups based on serial histological sections of peripheral nerves

The 3D reconstruction of the internal functional fascicular groups based on serial histological sections of peripheral nerves is currently a hot research topic. It has been shown that serial histological nerve section images are more precise and accurate than those obtained by microsection. The earliest research in this field was carried out by Chen et al. (2003), who performed 3D reconstruction of the brachial plexus.

Zhong et al. (2010) successfully performed 3D reconstruction of functional fascicular groups in short segments of the common peroneal nerve. The models were quite clear and stereoscopic (Zhang et al., 2009).

However, because there are technical problems, such as the acquisition of panoramic images, acquisition of location spots, registration and segmentation, mature imaging techniques such as CT, MRI and laser scan cannot reveal detailed information on the nerve stem.

Key technical problems in 3D reconstruction of functional fascicular groups inside the peripheral nerve

Acquisition of the marker: Locating the marker is a primary problem (Baheerathan et al., 1998). Human hair is considered the most suitable locating material (Zhang et al., 1999). However, we found that the adhesion of human hair was not satisfactory, and it could not meet the demands of automatic registration by computer. We discovered that adhesion was better on slides, and therefore, re-imaging method and hand drawn location spots were combined with automatic image synthesis.

Acquisition of 2D panoramic images: Another technical problem in this study was the acquisition of 2D panoramic images. Currently, digital scanning and micrographs are the two main methods for obtaining 2D images of the sections. The former can only produce lower resolution images, while the latter can produce higher resolution images; however, it is difficult to obtain complete panoramic images, because only one photograph can be placed at a time under a high-magnification microscope, limiting the processing of photographs and leading to inaccuracy.

In this study, 2D panoramic images of nerve sections were obtained on an Olympus Z61 stereomicroscope combined with MSHOT MD90 digital imaging equipment. The obtained image mosaic displayed a clear contour of the peripheral nerves, which made discrimination of peripheral groups easy. The simple procedure and accurate images suggest that it is a practical way to obtain 2D panoramic images.

Automatic registration and segmentation: Registration includes correctly shifting (Hibbard et al., 1993; Ross et al., 1994), rotating and transforming the slices, which depends on the locating spots. Two key problems need to be solved for automatic registration. One is searching and recognizing the locating spots in the microsection images. The other is correcting the images. In this study, we used the dynamic clustering algorithm for integration pattern recognition that could support vector machine theory. We also used an improved genetic algorithm for parameter optimization and studied artificial intelligent registration of the microscopic images of peripheral nerve sections in the realization of 3D visualization of peripheral nerves. To resolve the first key problem, we adopted optimized LS–SVM, which is easy to use and can recognize round objects. Even if there are a few pixels outside the template, recognition of the borderline is not affected. Consequently, accuracy and efficacy were enhanced (Sahoo et al., 1988). For the second key problem, conic calibration was used to correct image distortion, which has been a norm in fields such as industrial image correction.

Segmentation refers to the splitting of target objects from a complex background. The 2D images of peripheral nerves obtained by current technologies have various problems, including small variations in grayscales and irregular contour information. A satisfactory result is difficult to obtain with any one segmentation method alone (Chen, 2013). To solve the problem of non-consecutive borderlines in images of functional fascicles of the peripheral nerve, a dynamic clustering algorithm was used to process the images. We managed to cluster pixels with a similar grayscale in the center of the images into separate groups. With the encroaching technique, a designated pixel in the center of a functional fascicle of a peripheral nerve could be enlarged into an area encompassing the whole fascicle without crossing over the border. Consequently, we acquired a relatively precise borderline of functional fascicles. Because the dynamic clustering algorithm does not need the user to indicate the number of groups to be separated or the center of a group, it has been used successfully in areas such as image segmentation.

For the classification of the functional groups inside nerves, a relatively advanced method at present is micro-Raman spectrum analysis, which can be used to study and analyze the specific structures of peripheral nerve fascicles to obtain specific features of tissues, such as motor fascicles and sensory fascicles (Wang et al., 2006). Nevertheless, there is currently no published report on automatic Raman spectrum recognition. This technique requires further exploration.

Software applied in the 3D reconstruction of the peripheral nerve

Currently, there is no suitable software that can meet the demand of 3D reconstruction of peripheral nerves. Amira 4.1 software, newly developed by the French company TGS, is a 3D visualization and reconstruction software that has been widely used in varies fields, such as biomedicine, material science, physical geography and engineering, because of its effectiveness in reconstruction (Xu et al., 2007; Yang et al., 2007). Using Amira 4.1 software, we achieved the 3D

reconstruction of functional fascicular groups of a long ulnar nerve segment from the upper arm. Amira 4.1 software can directly input color images in different formats and automatically change them into images in grayscale. This simplifies 2D image pre-processing. Moreover, the software includes a built-in program to split images so that contour outlining can be done inside Amira 4.1 software. The software can automatically smoothen the zigzag effect produced by stacking consecutive slices and the variation of contours of matching objects in different slices to help reduce matching errors in section images of peripheral nerves. It is very suitable for nonrigid slice images of nerves and can dramatically simplify the process of 3D reconstruction. However, Amira 4.1 failed to resolve the segmentation problem of insignificant contrast in grayscale between peripheral nerves and surrounding soft tissue, and therefore, channel segmentation still had to be realized by manually marking the functional fascicular groups with different grayscales. Because the manual work is time-consuming, and inevitably leads to human errors, a more efficient and reliable automatic segmentation method is urgently needed.

In addition to the key technical problems that need to be solved, 3D reconstruction of human peripheral nerves has to be performed quickly, efficiently and accurately. Our results should help in the development of a digital system for visualizing the microstructure of peripheral nerves and help advance the treatment of peripheral nerve defects and injuries.

Author contributions: *JQ was responsible for nerve acquisition and experiment implementation. YCZ and XLL designed the study and XLL provided technical guidance. WYW and YZ operated re-imaging technique, implemented auto-registration and artificial recognition of nerve bundles. PL and CFH were responsible for specimen sectioning and histological staining. PT was in charge of development of automatic segmentation algorithm of nerve bundles. JMZ established the three-dimensional model. WYW and SZ participated in data collection. JQ and YZ finished writing the paper and WYW revised the paper. All authors approved the final version of the paper.*
Conflicts of interest: *None declared.*
Financial support: *This study was supported by the National Natural Science Foundation of China, No. 30571913; a grant from the Science and Technology Project of Guangdong Province of China, No. 2013B010404019; the Natural Science Foundation of Guangdong Province of China, No. 9151008901000006; the Medical Scientific Research Foundation of Guangdong Province of China, No. A2009173. The funders did not participant in the study design, in the collection, analysis and interpretation of data, in the writing of the paper, and in the decision to submit the paper for publication.*
Institutional review board statement: *The study protocol was approved by the First Affiliated Hospital of Sun Yat-sen University of (approval number: [2013]A-065).*
Copyright license agreement: *The Copyright License Agreement has been signed by all authors before publication.*
Data sharing statement: *Datasets analyzed during the current study are available from the corresponding author on reasonable request.*
Plagiarism check: *Checked twice by iThenticate.*
Peer review: *Externally peer reviewed.*

References

Baheerathan S, Albregtsen F, Danielsen HE (1998) Registration of serial sections of mouse liver cell nuclei. J Microsc 192:37-53.
Chen CH (2013) Pattern recognition and artificial intelligence. Salt Lake City: Academic Press, USA.
Chen ZG, Zhang M, Zhang J, Chen TY, Xia Q, Xie SS, Ping HU, Hua L (2008) Three-dimensional reconstruction of human sciatic nerve from serial tissue sections. Fudan Daxue Xuebao Yixue Ban 35:510-513.
Chen ZG, Zhang J, Chen T (2003) Three-dimensional reconstruction of brachial plexus inferior trunk from serial tissue sections. Zhongguo Linchuang Yixue Zazhi 10:133-135.
Hibbard LS, Grothe RJ, Arnicar-Sulze TL, Dovey-Hartman BJ, Page RB (1993) Computed three-dimensional reconstruction of median-eminence capillary modules: image alignment and correlation. J Microsc 171:39-56.
Jing LI, Yang X, Yu JP (2007) Medical MRI image registration based on the feature space. Zhongguo Tuxiang Tuxing Xuebao 12:1069-1078.
Lin Y, Tian J (2002) A survey on medical image segmentation methods. Moshi Shibie yu Rengong Zhineng 15:192-204.
Liu T, Hu P, Zhang J, Zhang M, Li H, Chen Z, Chen T, Chen Z (2008) 3D visualization research on microstructure of human ulnar nerve. Zhongguo Xiu Fu Chong Jian Wai Ke Za Zhi 22:1026-1030.
Pommert A, Hohne KH, Burmester E, Gehrmann S, Leuwer R, Petersik A, Pflesser B, Tiede U (2006) Computer-based anatomy a prerequisite for computer-assisted radiology and surgery. Acad Radiol 13:104-112.
Ren G, Pei G (2009) Research progress on three-dimensional reconstruction and visualization of peripheral nerve. Zhongguo Xiu Fu Chong Jian Wai Ke Za Zhi 23:239-244.
Ross MD, Cheng R, Doshay DG, Linton SW, Montgomery K, Parnas BR (1994) High performance computing applications in neurobiological research. Simulation Councils, Inc.
Sahoo PK, Soltani S, Wong AK (1988) A survey of thresholding techniques. Computer vision, graphics, and image processing 41:233-260.
Su XY, Pei GX, Yu B, Hu YL, Li J, Huang Q, Li X, Zhang YZ (2007) Landmark-based automatic registration of serial cross-sectional images of Chinese digital human using Photoshop and Matlab software. Nan Fang Yi Ke Da Xue Xue Bao 27:1884-1887.
Sun K, Zhang J, Chen T, Chen Z, Chen Z, Li Z, Li H, Hu P (2009) Three-dimensional reconstruction and visualization of the median nerve from serial tissue sections. Microsurg 29:573-577.
Wang H, Lu LJ, Kong XG, Liu DX, Ma FY (2006) Identification of the nature of peripheral nerve bundles with micro raman spectrum. Zhongguo Linchuang Kangfu 10:104-106.
Xu K, Pei G, Zhang Y (2007) Design of three-dimensional visualization for lateral flaps of legs based on the operational platform of Amira software. Jiefangjun Yixue Zazhi 32:701-703.
Yang P, Zhang SF, Liu JP, Zhou B, Meng QY (2007) Construction of a three-dimensional finite element analysis model of mandi-bular molars with Amira, UG and ALGOR softwares. Disi Junyi Daxue Xuebao 28:852-854.
Zhang W, Li S, Dai R (1999) Progress in technique of computer for three dimensional reconstruction from biological tissue series slices images. Sheng Wu Yi Xue Gong Cheng Xue Za Zhi 16:377-381.
Zhang Y, Qi J, Liu X, Xiong Z, Li S, Zhou J, Liang Y (2009) Three-dimensional reconstruction of functional fascicular groups inside a segment of common peroneal nerve. J Bioact Compat Pol 24:100-112.
Zhong Y, Zhang Y (2008) Recognition study on positioning line transection of nerve slice image. Jisuanji Gongcheng yu Yingyong 1:413-417.

(Copyedited by Patel B, Pack M, Wang J, Li CH, Qiu Y, Song LP, Zhao M)